

# Targeting Human Telomeric Higher-Order DNA: Dimeric G-Quadruplex Units Serve as Preferred Binding Site

Chuanqi Zhao,<sup>†</sup> Li Wu,<sup>†</sup> Jinsong Ren,<sup>†</sup> Yan Xu,<sup>‡</sup> and Xiaogang Qu<sup>\*†</sup>

<sup>†</sup>Division of Biological Inorganic Chemistry, State Key Laboratory of Rare Earth Resource Utilization and Laboratory of Chemical Biology, Changchun Institute of Applied Chemistry, Chinese Academy of Sciences, Changchun, Jilin 130022, China

<sup>‡</sup>Division of Chemistry, Department of Medical Sciences, Faculty of Medicine, University of Miyazaki, 5200 Kihara, Kiyotake, Miyazaki 889-1692, Japan

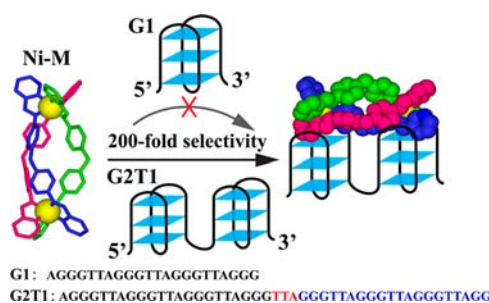
**S** Supporting Information

**ABSTRACT:** Long human telomeric fragments can form stable, higher-order G-quadruplex structures, recently identified in human cells, which are potential drug targets. However, there are very few examples of ligand binding to higher-order G-quadruplexes, and all the reported ligands are proposed to bind at the cleft between two G-quadruplexes. Here we report that zinc-finger-like chiral supramolecular complexes prefer binding to higher-order G-quadruplexes over a single G-quadruplex, with ~200-fold higher selectivity. To our knowledge, this is the first example of a ligand that can distinguish higher-order G-quadruplexes from a single G-quadruplex with such high selectivity. Further studies indicate that the nanosized chiral complex would bind to two well-matched G-quadruplex units, instead of binding at the cleft between the two G-quadruplexes. These results provide new insights into the targeting of higher-order G-quadruplex ligands. Our work illustrates that dimeric G-quadruplex units can be ligand-preferred binding sites.

Telomere structures are essential for eukaryotic chromosomes that contain highly repetitive guanine (G)-rich DNA sequences. In humans, telomeric DNA consists of a duplex region composed of hundreds of TTAGGG repeats, ending in a shorter G-rich single-stranded protrusion, which can fold into unique, highly stable four-stranded helices known as G-quadruplexes.<sup>1</sup> Recent studies demonstrate that G-quadruplex structures are stable and detectable in human cells.<sup>2</sup> G-quadruplexes participate in several key biological events, especially those that are aging-associated and disease-related.<sup>3</sup> They are involved in the activity regulation of telomerase, which is activated in 80–90% of human tumors and can serve as specific tumor-selective targets for chemotherapy.<sup>4</sup> Thus, compounds which can stabilize human telomeric G-quadruplex can be potential anticancer agents.<sup>5</sup>

A G-quadruplex monomer formed by short human telomeric DNA sequences (typically 21–26 nt) is usually used as the model to screen G-quadruplex-interactive ligands, as its high-resolution structure is well characterized by X-ray crystallography and NMR.<sup>6</sup> Since the telomeric terminal overhang is ~200 nt, it can form more-complex, higher-order G-quadruplex structures (dimer or multimer), consisting of consecutive G-quadruplex units connected by TTA linkers.<sup>7</sup> Compared with G-quadruplex

## Scheme 1. Preferred Binding of a Chiral Metallo-supramolecular Complex to a Higher-Order Dimeric G-Quadruplex over a Monomeric G-Quadruplex Unit



monomers, the higher-order G-quadruplex structure<sup>8</sup> is more biologically relevant, and the multimeric quadruplex units can be a predominant factor in recognizing long telomeric DNA in vivo. Thus, deciphering how ligands bind to long telomeric DNA is essential. Until now, most studies focused on ligand binding to monomeric G-quadruplexes. There are very few reports of ligand binding to higher-order G-quadruplexes,<sup>9</sup> as recently reviewed by Petraccone.<sup>9a</sup> In all the reported examples, the ligands are proposed to bind at the cleft between two consecutive G-quadruplexes. There is no report of a ligand binding to dimeric G-quadruplex units rather than binding monomeric G-quadruplexes. More importantly, since monomeric G-quadruplexes are known to be binding sites for ligands bound to single G-quadruplex DNA, dimeric G-quadruplex units are also potential targets for large ligand binding to higher-order G-quadruplexes.

Recently, our group reported that a zinc-finger-like nanosized chiral metallo-supramolecular complex, *P*-[Ni<sub>2</sub>L<sub>3</sub>]<sup>4+</sup> (Ni-P), displayed chiral and steric selectivity in stabilizing human telomeric monomeric G-quadruplex.<sup>10</sup> However, its enantiomer, *M*-[Ni<sub>2</sub>L<sub>3</sub>]<sup>4+</sup> (Ni-M), showed no specific binding with the monomeric G-quadruplex (Figures S1 and S2). The increasing interest in long telomeric DNA prompted us to study the binding properties of these chiral supramolecular complexes with higher-order G-quadruplexes. Here we report that Ni-M can bind to higher-order G-quadruplexes (dimeric G-quadruplexes) 200-fold better than to monomeric G-quadruplex (Scheme 1). In contrast to all the reported ligands, which bind to the cleft

Received: October 25, 2013

Published: November 22, 2013

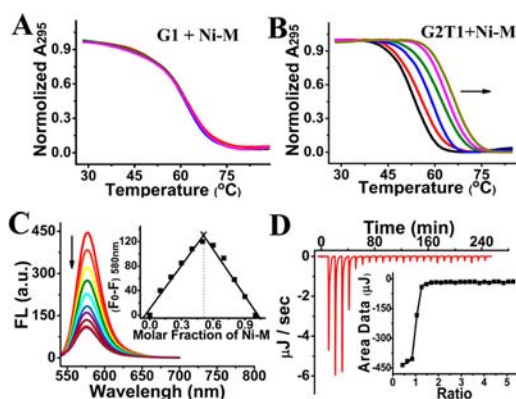


**Figure 1.** UV melting profiles of (A) G1 and (B) G2T1 in the absence and presence of Ni-M. Absorbance changes were measured at 295 nm. DNA concentration was  $2 \mu\text{M}$  in strand, and Ni-M concentration ranged from  $0.5$  to  $4 \mu\text{M}$ . (C) Fluorescence emission spectra of TMR-G2T1 titrated by Ni-M,  $\lambda_{\text{ex}} = 480 \text{ nm}$ . Inset: Job's plot for complexation of Ni-M with TMR-G2T1.  $[\text{Ni-M}] + [\text{TMR-G2T1}] = 0.3 \mu\text{M}$ ,  $\lambda_{\text{ex}} = 480 \text{ nm}$ . (D) Representative ITC profile for the titration of Ni-M into a solution of G2T1, and (inset) the corresponding normalized heat signals versus molar ratio. All the experiments were carried out in  $10 \text{ mM}$  Tris-HCl buffer,  $100 \text{ mM}$  NaCl, pH 7.2.

between the two G-quadruplexes,<sup>9</sup> the nanosized chiral metallo-supramolecular complex would bind to the well-matched two G-quadruplex units. To the best of our knowledge, this is the first example that a ligand can distinguish higher-order G-quadruplexes from single G-quadruplexes with such a huge difference. These results will facilitate design of ligands targeting higher-order G-quadruplexes, and indicate that dimeric G-quadruplex units can be preferred binding sites.

On the basis of previous reports,<sup>7,8</sup> we chose a dimeric G-quadruplex (named G2T1) as the higher-order structure to compare its ligand-binding properties with those of a monomeric G-quadruplex (named G1). It should be noted that human telomeric G-quadruplex structures are highly polymorphic. The "real" structure for the long human telomeric sequence in  $\text{K}^+$  solution is still an open question.<sup>9a</sup> In contrast, the conformation of high-order G-quadruplexes in  $\text{Na}^+$  solution is clear.<sup>8b</sup> Thus, we chose  $\text{Na}^+$  buffer to carry out our experiments.<sup>6b,11</sup>

DNA UV melting studies<sup>12</sup> clearly indicated that Ni-M showed negligible influence on the melting temperature ( $T_m$ ) of G1 (Figure 1A), whereas it significantly increased the  $T_m$  of G2T1 (Figures 1B and S3), demonstrating that Ni-M specifically bound to high-order G2T1 over G1. By plotting the variations of DNA melting temperature as a function of complex concentration (Figure S4), we observed a 1:1 binding ratio for Ni-M binding with G2T1. The binding stoichiometry was further confirmed through titrating fluorescent TMR-labeled G2T1 by Ni-M (Ni-M could quench the fluorescence of TMR-labeled DNA owing to a possible electron-transfer mechanism, as shown in Figure S5). Clearly, the results of both the titration curve (Figure S6) and Job's plot (Figure 1C, inset) illustrate 1:1 binding between Ni-M and G2T1. In addition, the 1:1 binding between Ni-M and G2T1 was verified by isothermal titration calorimetry (ITC, Figure 1D).

To verify the selectivity of Ni-M for G2T1 over G1, native gel electrophoresis experiments were performed. We previously reported that Ni-P can bind to G1 monomer but Ni-M cannot.<sup>10a</sup> In Figure 2A, in the presence of Ni-P, a new retarded band is observed due to formation of Ni-P-G1 complex, whereas no new band is observed for G1 incubated with Ni-M, indicating that Ni-

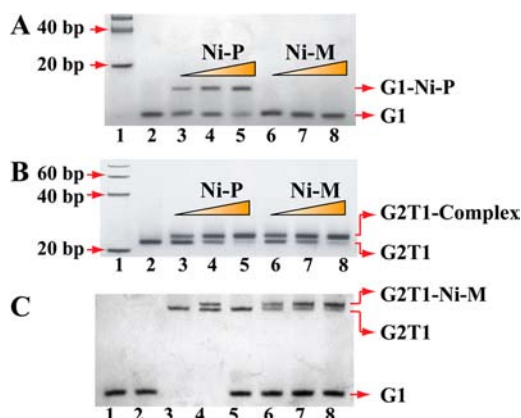


**Figure 2.** Native gel electrophoretic analysis of (A) G1 and (B) G2T1 in the presence of various concentrations of Ni-M and Ni-P: lane 1, DNA marker; lane 2, DNA alone; lanes 3–5, DNA with Ni-P at ratios of 2:1, 1:1, and 2:3, respectively; lanes 6–8, DNA with Ni-M at ratios of 2:1, 1:1, and 2:3, respectively. (C) Native gel electrophoretic analysis of the mixture of G1 and G2T1: lanes 1 and 2, G1 in the absence and presence of Ni-M, respectively; lanes 3 and 4, G2T1 in the absence and presence of Ni-M, respectively; lane 5, mixture of G1 and G2T1; lanes 6–8, mixtures of G1 ( $10 \mu\text{M}$ ) and G2T1 ( $5 \mu\text{M}$ ) in the presence of 4, 8, and  $12 \mu\text{M}$  Ni-M, respectively. Each band is illustrated to the right of the electropherogram. Gels were run in TB buffer with  $10 \text{ mM}$  NaCl at  $4 \text{ }^\circ\text{C}$ .

M did not form a stable complex with G1. In contrast, for G2T1, both Ni-M and Ni-P led to new retarded bands, ascribed to formation of Ni-M/Ni-P-G2T1 complex (Figure 2B). These results clearly reveal that Ni-M selectively binds to G2T1 instead of G1. Note that nearly 100% of the G2T1 sequence could form the higher-order structure under the experimental conditions (lane 2 in Figure 2B and Figure S7). To further certify this selectivity, Ni-M was incubated with a mixture of G2T1 and G1. Obviously, G1 and G2T1 formed intramolecular monomeric G-quadruplex or dimeric G-quadruplex, respectively, without disturbing each other (Figure 2C, lane 5).<sup>13</sup> After addition of Ni-M to the mixture of G2T1 and G1, a new retarded band corresponding to Ni-M-G2T1 complex appeared (Figure 2C, lanes 6–8). These results imply that, even while coexisting with G2T1 and G1, Ni-M can selectively bind to G2T1 owing to its high binding affinity with G2T1, in agreement with the melting results.

Competitive binding assays and fluorescence stopped-flow kinetic studies were next carried out to verify the stronger binding of Ni-M to G2T1. As shown in Figure 3A, Ni-M just slightly decreases the fluorescence of TMR-G1, due to the

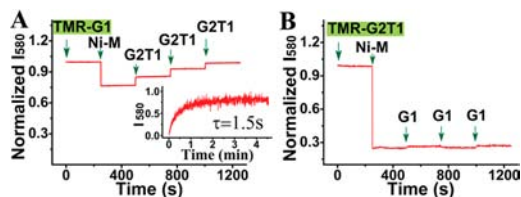


**Figure 3.** (A) Normalized fluorescence intensity change of TMR-G1 ( $0.3 \mu\text{M}$ ) with orderly addition of Ni-M ( $0.3 \mu\text{M}$ ) and G2T1 ( $0.15 \mu\text{M}$  every time) as indicated. Inset: Stopped-flow study of the competition binding of Ni-M between G1 and G2T1. (B) Normalized fluorescence intensity change of TMR-G2T1 ( $0.3 \mu\text{M}$ ) with orderly addition of Ni-M ( $0.3 \mu\text{M}$ ) and G1 ( $0.3 \mu\text{M}$  every time) as indicated. Fluorescence was monitored at  $580 \text{ nm}$  with  $\lambda_{\text{ex}} = 480 \text{ nm}$ . Experiments carried out in  $10 \text{ mM}$  Tris-HCl buffer,  $100 \text{ mM}$  NaCl, pH 7.2.

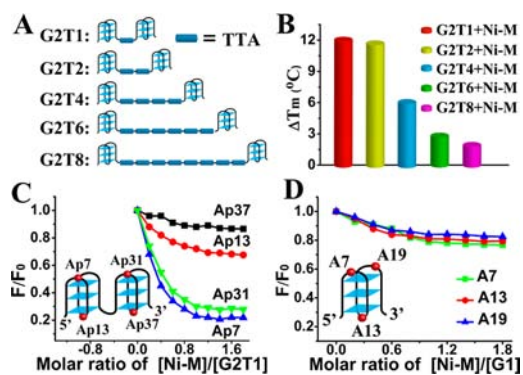


**Figure 4.** (A) Schematic structure of various dimeric G-quadruplexes with different length linkers. (B) Variations of the melting temperature of various dimeric G-quadruplexes induced by Ni-M binding. (C) Plot of normalized fluorescence intensity at 370 nm of 2-Ap individually labeled G2T1 versus binding ratio of Ni-M/[G2T1]. Inset: illustration of the 2-Ap position in G2T1. (D) Plot of normalized fluorescence intensity at 370 nm of 2-Ap individually labeled G1 versus binding ratio of Ni-M/[G1]. Inset: illustration of the 2-Ap position in G1. Experiments carried out in 100 mM NaCl, 10 mM Tris buffer, pH 7.2.

nonspecific electrostatic binding. After addition of G2T1 to the solution of Ni-M and TMR-G1, the fluorescence of TMR-G1 is rapidly restored, indicating that G2T1 could competitively bind to Ni-M and form a more stable complex, leading to the fluorescence recovery of TMR-G1. Fluorescence stopped-flow kinetic studies (Figure 3A, inset) show that the displacement process was completed in <1.5 s. In contrast, G1 exhibits no influence on the mixture of TMR-G2T1 and Ni-M (Figure 3B). These results unambiguously illustrate that Ni-M bound much more strongly to G2T1 than to G1.

As analyzed above, Ni-M interacts with G2T1 in a 1:1 stoichiometry. Thus, we speculated that one Ni-M might simultaneously interact with the two G-quadruplex subunits of G2T1. To verify this, a series of dimeric G-quadruplexes with different length linkers ranging from 1 to 8 TTAs were designed and interacted with Ni-M (Figure 4A). If one Ni-M bound to two G-quadruplex motifs simultaneously, a short TTA linker would favor its binding. Accordingly, the long TTA linkers would hamper the binding because of the increasing spatial distance between the two G-quadruplex units. As expected, with linkers getting longer, the stabilization effect of Ni-M on dimeric G-quadruplexes became weaker (Figures 4B and S8). These results support the above speculation that one Ni-M interacts with the two G-quadruplex units in G2T1. Because the G-quartet was  $\sim 1.1$  nm in width<sup>14</sup> and the TTA linker was flexible, the distance from the center of one G-quartet plane to the center of another G-quartet was considered to be larger than 1.1 nm. Coincidentally, Ni-M was  $\sim 1.15$  nm in length between two nickel atoms, with diameter of 0.8 nm.<sup>15</sup> Thus, stacking on the end G-quartets of the two G-quadruplex motifs might be its favored DNA-binding mode (Scheme 1), which would provide a beneficial effect on shape recognition and electrostatic interactions between Ni-M and G2T1.

Modification of 2-aminopurine (2-Ap) in different loops was widely used to estimate the ligand binding mode with quadruplex DNA.<sup>16</sup> To further examine the stacking mode of Ni-M on G2T1 DNA, we performed fluorescence experiments using G2T1 with substitutions at adenine residue positions 7, 13, 31, and 37 (Figure 4C). It should be noted that, after interacting with Ni-M, G2T1 maintained its conformation, with both G-quadruplex

subunits still in the antiparallel structure (Figures S9–S11).<sup>10a,17</sup> Clearly, adding Ni-M to G2T1 significantly decreased the fluorescence of Ap7 and Ap31, whereas it only weakly affected the fluorescence of Ap13 and Ap37 (Figure 4C). This indicated that, after binding with G2T1, Ni-M has closer contacts with Ap7 and Ap31 than with Ap13 and Ap37. These results are understandable because the diagonal loops (Ap13 loop and Ap37 loop) would hinder Ni-M from stacking on the corresponding end G-quartets. The above results indicated that Ni-M may stack on the end G-quartets (G-quartet near Ap7 and G-quartet near Ap31) of the two G-quadruplex units in G2T1, as shown in Scheme 1 and Figure S12. Although no crystal or NMR structure of higher-order human telomeric G-quadruplexes is reported, and we did not get a binding model using molecular dynamics simulations because of the complexity of the metallo-supramolecular Ni-M (two Ni<sup>2+</sup>, a large molecular weight), our melting results, ITC assays, 2-Ap fluorescence studies, and competitive binding and fluorescence stopped-flow kinetic studies indicate that Ni-M could preferentially bind to the end G-quartets of G2T1 by external stacking. In this sense, dimeric G-quadruplex units can be novel potential targets for design of ligands targeting higher-order G-quadruplexes.

Nonlinear least-squares analysis of the fluorescence titration data of Ap7 by Ni-M yielded binding constants of  $4.6 \times 10^7$  M<sup>-1</sup> for G2T1 and just  $1.9 \times 10^5$  M<sup>-1</sup> for G1, as shown in Table 1. The

**Table 1. Binding Constants of Ni-M with G2T1 and G1<sup>a</sup>**

	<sup>1</sup> K <sub>a</sub> (M <sup>-1</sup> )	<sup>2</sup> K <sub>a</sub> (M <sup>-1</sup> )
G2T1	$4.6(\pm 0.8) \times 10^7$	$2.7(\pm 0.3) \times 10^7$
G1	$1.9(\pm 0.5) \times 10^5$	$1.1(\pm 0.4) \times 10^5$

<sup>a</sup>Binding constant <sup>1</sup>K<sub>a</sub> was measured by fluorescence titration method. Binding constant <sup>2</sup>K<sub>a</sub> was measured by ITC method. The values are the averages of two independent measurements. Experimental details are described in the Supporting Information.

results are in good agreement with the binding constants determined by ITC ( $2.7 \times 10^7$  M<sup>-1</sup> for G2T1 and  $1.1 \times 10^5$  M<sup>-1</sup> for G1). This indicates that binding of Ni-M to G2T1 was  $\sim 200$ -fold stronger than its binding to G1. This huge difference in binding affinity is consistent with melting, native gel electrophoresis, and competition binding results. To the best of our knowledge, there is no previous report of a ligand bearing such high affinity and excellent selectivity for higher-order G-quadruplexes over monomeric G-quadruplexes.

To further understand the selectivity of Ni-M between G2T1 and G1, the thermodynamic parameters for Ni-M binding to G2T1 and G1 were evaluated by ITC (Figures 1D and S13), and the data are listed in Table 2.<sup>18</sup> The results imply that Ni-M

**Table 2. Thermodynamic Parameters for the Interaction of Ni-M with G2T1 and G1<sup>a</sup>**

	G2T1	G1
<i>n</i>	$1.1 \pm 0.1$	$1.6 \pm 0.2$
$\Delta G^\circ_{25}$ (kcal mol <sup>-1</sup> )	$-10.1 \pm 0.2$	$-6.8 \pm 0.4$
$\Delta H^\circ$ (kcal mol <sup>-1</sup> )	$-19.9 \pm 0.8$	$-10.8 \pm 0.9$
$T\Delta S^\circ$ (kcal mol <sup>-1</sup> K <sup>-1</sup> )	$-9.8 \pm 0.4$	$-4.0 \pm 0.7$

<sup>a</sup>All data were derived from ITC experiments.  $\Delta H^\circ$  and *n* (stoichiometry) were directly obtained from ITC.  $\Delta G^\circ_{25}$  was obtained from the relation  $\Delta G^\circ = -RT \ln K_a$  (values for *K<sub>a</sub>* are listed in Table 1).  $T\Delta S^\circ$  was obtained from the relation  $T\Delta S^\circ = \Delta H^\circ - \Delta G^\circ$ . The values are the average of two independent measurements.

stabilizing G2T1 was due to a more favorable enthalpy contribution. We also obtained the binding parameters by melting analysis.<sup>8b,19</sup> The results indicate that the favorable enthalpy plays a key role in the binding between Ni-M and G2T1 (Figures S14–S16), in good accordance with the ITC results.

Binding of Ni-P, the enantiomer of Ni-M, to G2T1 or G1 was also studied. Like Ni-M, Ni-P exhibits stronger binding to G2T1 than to G1 (Figures S17–S19); it can be concluded that both Ni-M and Ni-P prefer binding to G2T1 over G1. The chiral selectivity of Ni-M and Ni-P in stabilizing G2T1 was also compared. DNA melting results show that Ni-P has a stronger stabilizing effect than Ni-M (Figure S20)—not surprising because Ni-P bound more tightly to G-quadruplex monomers than Ni-M.<sup>10a</sup> These results indicate that the chiral selectivity still existed when the two enantiomers bound to higher-order G-quadruplexes.

In summary, our results indicate that nanosized chiral supramolecular complexes prefer binding to higher-order G-quadruplexes over single G-quadruplex units with ~200-fold different selectivity. There is no report to show that a ligand can distinguish higher-order G-quadruplexes from single G-quadruplexes with such high selectivity. Unlike the few reported ligands which can bind to the cleft between the two G-quadruplexes, the nanosized chiral metallo-supramolecular complex would bind to two well-matched G-quadruplex units. Our work indicates that dimeric G-quadruplex units can be novel binding sites for large ligands targeting higher-order G-quadruplexes.

## ■ ASSOCIATED CONTENT

### Supporting Information

Experimental details and additional data. This material is available free of charge via the Internet at <http://pubs.acs.org>.

## ■ AUTHOR INFORMATION

### Corresponding Author

xqu@ciac.ac.cn

### Notes

The authors declare no competing financial interest.

## ■ ACKNOWLEDGMENTS

This work was supported by 973 Project (2011CB936004, 2012CB720602) and NSFC (21210002, 91213302, 21202158).

## ■ REFERENCES

- (1) (a) Bochman, M. L.; Paeschke, K.; Zakian, V. A. *Nat. Rev. Genet.* **2012**, *13*, 770. (b) Huppert, J. L. *Chem. Soc. Rev.* **2008**, *37*, 1375. (c) Murat, P.; Singh, Y.; Defrancq, E. *Chem. Soc. Rev.* **2011**, *40*, 5293. (d) Phong Lan Thao, T.; Mergny, J.-L.; Alberti, P. *Nucleic Acid Res.* **2011**, *39*, 3282.
- (2) (a) Siddiqui-Jain, A.; Hurley, L. H. *Nat. Chem.* **2013**, *5*, 153. (b) Biffi, G.; Tannahill, D.; McCafferty, J.; Balasubramanian, S. *Nat. Chem.* **2013**, *5*, 182. (c) Paeschke, K.; Simonsson, T.; Postberg, J.; Rhodes, D.; Lipps, H. J. *Nat. Struct. Mol. Biol.* **2005**, *12*, 847. (d) Lam, E. Y. N.; Beraldi, D.; Tannahill, D.; Balasubramanian, S. *Nat. Commun.* **2013**, *4*, 1796. (e) Xu, Y.; Komiyama, M. *ChemBiochem* **2013**, *14*, 927.
- (3) (a) Xu, Y. *Chem. Soc. Rev.* **2011**, *40*, 2719. (b) Ren, J.; Qu, X.; Trent, J. O.; Chaires, J. B. *Nucleic Acid Res.* **2002**, *30*, 2307. (c) O'Sullivan, R. J.; Karseder, J. *Nat. Rev. Mol. Cell. Biol.* **2010**, *11*, 171.
- (4) (a) Balasubramanian, S.; Hurley, L. H.; Neidle, S. *Nat. Rev. Drug Discov.* **2011**, *10*, 261. (b) Riou, J. F.; Guittat, L.; Mailliet, P.; Laoui, A.; Renou, E.; Petitgenet, O.; Megnin-Chanet, F.; Helene, C.; Mergny, J. L. *Proc. Natl. Acad. Sci. U.S.A.* **2002**, *99*, 2672.
- (5) (a) Read, M.; Harrison, R. J.; Romagnoli, B.; Tanius, F. A.; Gowan, S. H.; Reszka, A. P.; Wilson, W. D.; Kelland, L. R.; Neidle, S.

*Proc. Natl. Acad. Sci. U.S.A.* **2001**, *98*, 4844. (b) Kim, M.-Y.; Vankayalapati, H.; Shin-ya, K.; Wierzbka, K.; Hurley, L. H. *J. Am. Chem. Soc.* **2002**, *124*, 2098. (c) Bejugam, M.; Sewitz, S.; Shirude, P. S.; Rodriguez, R.; Shahid, R.; Balasubramanian, S. *J. Am. Chem. Soc.* **2007**, *129*, 12926. (d) Reed, J. E.; Arnal, A. A.; Neidle, S.; Vilar, R. *J. Am. Chem. Soc.* **2006**, *128*, 5992.

(6) (a) Parkinson, G. N.; Lee, M. P. H.; Neidle, S. *Nature* **2002**, *417*, 876. (b) Wang, Y.; Patel, D. J. *Structure* **1993**, *1*, 263. (c) Lim, K. W.; Amrane, S.; Bouaziz, S.; Xu, W.; Mu, Y.; Patel, D. J.; Luu, K. N.; Phan, A. T. N. *J. Am. Chem. Soc.* **2009**, *131*, 4301. (d) Phan, A. T.; Kuryavyi, V.; Luu, K. N.; Patel, D. J. *Nucleic Acid Res.* **2007**, *35*, 6517. (e) Zhang, Z.; Dai, J.; Veliath, E.; Jones, R. A.; Yang, D. *Nucleic Acids Res.* **2010**, *38*, 1009. (f) Ambrus, A.; Chen, D.; Dai, J. X.; Bialis, T.; Jones, R. A.; Yang, D. Z. *Nucleic Acid Res.* **2006**, *34*, 2723. (g) Mashimo, T.; Yagi, H.; Sannohe, Y.; Rajendran, A.; Sugiyama, H. *J. Am. Chem. Soc.* **2010**, *132*, 14910. (h) Luu, K. N.; Phan, A. T.; Kuryavyi, V.; Lacroix, L.; Patel, D. J. *J. Am. Chem. Soc.* **2006**, *128*, 9963.

(7) (a) Xu, Y.; Ishizuka, T.; Kurabayashi, K.; Komiyama, M. *Angew. Chem., Int. Ed.* **2009**, *48*, 7833. (b) Petraccone, L.; Trent, J. O.; Chaires, J. B. *J. Am. Chem. Soc.* **2008**, *130*, 16530. (c) Petraccone, L.; Spink, C.; Trent, J. O.; Garbett, N. C.; Mekmaysy, C. S.; Giancola, C.; Chaires, J. B. *J. Am. Chem. Soc.* **2011**, *133*, 20951.

(8) (a) Amrane, S.; Adrian, M.; Heddi, B.; Serero, A.; Nicolas, A.; Mergny, J.-L.; Phan, A. T. *J. Am. Chem. Soc.* **2012**, *134*, 5807. (b) Yu, H.; Gu, X.; Nakano, S.-i.; Miyoshi, D.; Sugimoto, N. *J. Am. Chem. Soc.* **2012**, *134*, 20060. (c) Lue, N. F.; Zhou, R.; Chico, L.; Mao, N.; Steinberg-Neifach, O.; Ha, T. *PLoS Genet.* **2013**, *9*, e1003145. (d) Renciuik, D.; Kejnovska, I.; Skolakova, P.; Bednarova, K.; Motlova, J.; Vorlickova, M. *Nucleic Acids Res.* **2009**, *37*, 6625. (e) Haider, S.; Parkinson, G. N.; Neidle, S. *Biophys. J.* **2008**, *95*, 296. (f) Paul, A.; Jain, A. K.; Misra, S. K.; Maji, B.; Muniyappa, K.; Bhattacharya, S. *PLoS One* **2012**, *7*, e39467.

(9) (a) Petraccone, L. *Top. Curr. Chem.* **2013**, *330*, 23. (b) Shinohara, K.; Sannohe, Y.; Kaieda, S.; Tanaka, K.; Osuga, H.; Tahara, H.; Xu, Y.; Kawase, T.; Bando, T.; Sugiyama, H. *J. Am. Chem. Soc.* **2010**, *132*, 3778. (c) Stefan, L.; Denat, F.; Monchaud, D. *J. Am. Chem. Soc.* **2011**, *133*, 20405. (d) Cummaro, A.; Fotticchia, I.; Franceschin, M.; Giancola, C.; Petraccone, L. *Biochimie* **2011**, *93*, 1392. (e) Bai, L. P.; Hagihara, M.; Jiang, Z. H.; Nakatani, K. *ChemBioChem* **2008**, *9*, 2583.

(10) (a) Yu, H. J.; Wang, X. H.; Fu, M. L.; Ren, J. S.; Qu, X. *Nucleic Acid Res.* **2008**, *36*, S695. (b) Yu, H.; Zhao, C.; Chen, Y.; Fu, M.; Ren, J.; Qu, X. *J. Med. Chem.* **2009**, *53*, 492. (c) Zhao, C.; Geng, J.; Feng, L.; Ren, J.; Qu, X. *Chem.—Eur. J.* **2011**, *17*, 8209. (d) Yu, H.; Li, M.; Liu, G.; Geng, J.; Wang, J.; Ren, J.; Zhao, C.; Qu, X. *Chem. Sci.* **2012**, *3*, 3145.

(11) (a) Xu, Y.; Kaminaga, K.; Komiyama, M. *J. Am. Chem. Soc.* **2008**, *130*, 11179. (b) Gray, R. D.; Chaires, J. B. *Nucleic Acids Res.* **2008**, *36*, 4191. (c) Nicoludis, J. M.; Barrett, S. P.; Mergny, J.-L.; Yatsunyk, L. A. *Nucleic Acids Res.* **2012**, *40*, 5432.

(12) Zhao, C.; Ren, J.; Gregoliński, J.; Lisowski, J.; Qu, X. *Nucleic Acids Res.* **2012**, *40*, 8186.

(13) Pedroso, I. M.; Duarte, L. F.; Yanez, G.; Burkewitz, K.; Fletcher, T. M. *Biopolymers* **2007**, *87*, 74.

(14) De Cian, A.; DeLemos, E.; Mergny, J.-L.; Teulade-Fichou, M.-P.; Monchaud, D. *J. Am. Chem. Soc.* **2007**, *129*, 1856.

(15) Hannon, M. J.; Painting, C. L.; Hamblin, J.; Jackson, A.; Errington, W. *Chem. Commun.* **1997**, 1807.

(16) (a) Kimura, T.; Kawai, K.; Fujitsuka, M.; Majima, T. *Chem. Commun.* **2006**, 0, 401. (b) Li, X.; Peng, Y. H.; Ren, J.; Qu, X. *Proc. Natl. Acad. Sci. U.S.A.* **2006**, *103*, 19658. (c) Nagesh, N.; Buscaglia, R.; Dettler, J. M.; Lewis, E. A. *Biophys. J.* **2010**, *98*, 2628.

(17) (a) Vorlíčková, M.; Kejnovská, I.; Sagi, J.; Renčíuk, D.; Bednářová, K.; Motlová, J.; Kyrp, J. *Methods* **2012**, *57*, 64. (b) Hud, N. V.; Smith, F. W.; Anet, F. A. L.; Feigon, J. *Biochemistry* **1996**, *35*, 15383.

(18) Miyoshi, D.; Matsumura, S.; Nakano, S.; Sugimoto, N. *J. Am. Chem. Soc.* **2004**, *126*, 165.

(19) (a) Marky, L. A.; Breslauer, K. J. *Biopolymers* **1987**, *26*, 1601. (b) Yu, H.-Q.; Miyoshi, D.; Sugimoto, N. *J. Am. Chem. Soc.* **2006**, *128*, 15461. (c) Lannan, F. M.; Mamajanov, I.; Hud, N. V. *J. Am. Chem. Soc.* **2012**, *134*, 15324.